Large Extra Dimensions at High Energy Colliders

A.A. Pankov *, *A.V. Tsytrinov*

ICTP Affiliated Centre, Pavel Sukhoi

Gomel State Technical University, Gomel 246746, Belarus

Abstract

We explore the capability of the high energy colliders LHC and ILC to distinguish spin-2 Kaluza-Klein towers of gravitons exchange from other new physics effects which might be conveniently parametrized by the four-fermion contact interactions. We find that the LHC and ILC with planned energies and luminosities will be capable of discovering and identifying graviton exchange effects in the ADD scenario with the cutoff parameter of order 5-9 TeV depending on energy and luminosity.

1 Introduction

The concept of four-fermion contact interactions (CI) provides a convenient method to investigate the interference of any new particle field predicted by many types of new physics (NP) scenarios and associated to large scales Λ, with γ and Z fields of the Standard Model (SM). Some of these different scenarios are: composite models of quarks and leptons [1]; exchanges of heavy Z' [2] and (scalar and vector) leptoquarks [3]; R-parity breaking sneutrino exchange [4]; anomalous gauge boson couplings [5]; Kaluza–Klein graviton exchange, exchange of gauge boson KK towers or string excitations, *etc.* [6]. There is a hope that new physics effects will be observed either directly, as in the case of new particle production, e.g., Z' and W' vector bosons, SUSY or Kaluza-Klein (KK) resonances, or indirectly through deviations, from the SM predictions, of observables such as cross sections and asymmetries.

*E-mail: pankov@ictp.it

Over the last years, intensive studies have been carried out, of how different scenarios involving extra dimensions would manifest themselves at high energy colliders such as the Large Hadron Collider (LHC) and an e^+e^- International Linear Collider (ILC) [6]. We shall consider the possibility of distinguishing such effects of extra dimensions from other NP scenarios at ILC and LHC, focusing on a model with large extra dimensions, namely the Arkani-Hamed–Dimopoulos–Dvali (ADD) [7] scenario.

Here, we consider as basic observables the differential cross sections for the fermion pair production processes

$$e^+ + e^- \to \bar{f} + f, \qquad (f = e, \mu, \tau, c, b) \tag{1}$$

at the International Linear Collider (ILC) with longitudinally polarized electron and positron beams and the lepton pair production process

$$p + p \to l^+ l^- + X. \tag{2}$$

at the LHC.

2 Virtual graviton exchange at ILC

2.1 Polarized differential observables

The expression of the polarized differential cross section for the process $e^+e^- \to f\bar{f}$ with $f \neq e, t$ and in approximation where $m_f << \sqrt{s}$ can be expressed as [8]:

$$\begin{aligned} \frac{d\sigma(P^-, P^+)}{dz} &= \frac{D}{4}[(1 - P_{\text{eff}})\left(\frac{d\sigma_{\text{LL}}}{dz} + \frac{d\sigma_{\text{LR}}}{dz}\right) + \\ &+(1 + P_{\text{eff}})\left(\frac{d\sigma_{\text{RR}}}{dz} + \frac{d\sigma_{\text{RL}}}{dz}\right)]. \end{aligned} \tag{3}$$

In Eq. (4), $z = \cos\theta$ with θ the angle between initial and final fermions in the C.M. frame, and the subscripts L, R denote the respective helicities. Furthermore, with P^- and P^+ denoting the degrees of longitudinal polarization of the e^- and e^+ beams, respectively, one has

$$D = 1 - P^- P^+, \qquad P_{\text{eff}} = \frac{P^- - P^+}{1 - P^- P^+}. \tag{4}$$

The SM amplitudes for these processes are determined by γ and Z exchanges in the s-channel.

The polarized differential cross section for the Bhabha process $e^+e^- \to e^+e^-$, where γ and Z can be exchanged also in the t-channel, can be conveniently written as [9, 10, 11]:

$$\frac{\mathrm{d}\sigma(P^-,P^+)}{\mathrm{d}z} = \frac{(1+P^-)(1-P^+)}{4}\frac{\mathrm{d}\sigma_{\mathrm{R}}}{\mathrm{d}z} + \frac{(1-P^-)(1+P^+)}{4}\frac{\mathrm{d}\sigma_{\mathrm{L}}}{\mathrm{d}z}$$
$$+\frac{(1+P^-)(1+P^+)}{4}\frac{\mathrm{d}\sigma_{\mathrm{RL},t}}{\mathrm{d}z} + \frac{(1-P^-)(1-P^+)}{4}\frac{\mathrm{d}\sigma_{\mathrm{LR},t}}{\mathrm{d}z}, \qquad (5)$$

with the decomposition

$$\frac{\mathrm{d}\sigma_{\mathrm{L}}}{\mathrm{d}z} = \frac{\mathrm{d}\sigma_{\mathrm{LL}}}{\mathrm{d}z} + \frac{\mathrm{d}\sigma_{\mathrm{LR},s}}{\mathrm{d}z}, \qquad \frac{\mathrm{d}\sigma_{\mathrm{R}}}{\mathrm{d}z} = \frac{\mathrm{d}\sigma_{\mathrm{RR}}}{\mathrm{d}z} + \frac{\mathrm{d}\sigma_{\mathrm{RL},s}}{\mathrm{d}z}. \qquad (6)$$

In Eqs. (5) and (6), the subscripts t and s denote helicity cross sections with SM γ and Z exchanges in the corresponding channels. In terms of helicity amplitudes:

$$\frac{\mathrm{d}\sigma_{\mathrm{LR},t}}{\mathrm{d}z} = \frac{\mathrm{d}\sigma_{\mathrm{RL},t}}{\mathrm{d}z} = \frac{2\pi\alpha^2_{\mathrm{e.m.}}}{s}\left|G_{\mathrm{LR},t}\right|^2, \quad \frac{\mathrm{d}\sigma_{\mathrm{LR},s}}{\mathrm{d}z} = \frac{\mathrm{d}\sigma_{\mathrm{RL},s}}{\mathrm{d}z} = \frac{2\pi\alpha^2_{\mathrm{e.m.}}}{s}\left|G_{\mathrm{LR},s}\right|^2,$$

$$\frac{\mathrm{d}\sigma_{\mathrm{LL}}}{\mathrm{d}z} = \frac{2\pi\alpha^2_{\mathrm{e.m.}}}{s}\left|G_{\mathrm{LL},s}+G_{\mathrm{LL},t}\right|^2, \quad \frac{\mathrm{d}\sigma_{\mathrm{RR}}}{\mathrm{d}z} = \frac{2\pi\alpha^2_{\mathrm{e.m.}}}{s}\left|G_{\mathrm{RR},s}+G_{\mathrm{RR},t}\right|^2. \qquad (7)$$

The polarized differential cross section (4) for the leptonic channels $e^+e^- \to l^+l^-$ with $l = \mu, \tau$ can be obtained directly from Eq. (5), basically by dropping the t-channel poles. The same is true, after some obvious adjustments, for the $\bar{c}c$ and $\bar{b}b$ final states.

According to the previous considerations the amplitudes $G_{\alpha\beta,i}$, with $\alpha,\beta = \mathrm{L},\mathrm{R}$ and $i = s,t$, are given by the sum of the SM γ, Z exchanges plus deviations representing the effect of the novel, contactlike, effective interactions:

$$
\begin{aligned}
G_{\mathrm{LL},s} &= u\left(\frac{1}{s}+\frac{g_{\mathrm{L}}^2}{s-M_Z^2}+\Delta_{\mathrm{LL},s}\right),\\
G_{\mathrm{LL},t} &= u\left(\frac{1}{t}+\frac{g_{\mathrm{L}}^2}{t-M_Z^2}+\Delta_{\mathrm{LL},t}\right),\\
G_{\mathrm{RR},s} &= u\left(\frac{1}{s}+\frac{g_{\mathrm{R}}^2}{s-M_Z^2}+\Delta_{\mathrm{RR},s}\right),\\
G_{\mathrm{RR},t} &= u\left(\frac{1}{t}+\frac{g_{\mathrm{R}}^2}{t-M_Z^2}+\Delta_{\mathrm{RR},t}\right),\\
G_{\mathrm{LR},s} &= t\left(\frac{1}{s}+\frac{g_{\mathrm{R}}\,g_{\mathrm{L}}}{s-M_Z^2}+\Delta_{\mathrm{LR},s}\right),\\
G_{\mathrm{LR},t} &= s\left(\frac{1}{t}+\frac{g_{\mathrm{R}}\,g_{\mathrm{L}}}{t-M_Z^2}+\Delta_{\mathrm{LR},t}\right).
\end{aligned}
\tag{8}
$$

Here $u,t=-s(1\pm z)/2$, $g_{\mathrm{R}}=\tan\theta_W$ and $g_{\mathrm{L}}=-\cot 2\,\theta_W$ with θ_W the electroweak mixing angle. The deviations $\Delta_{\alpha\beta,i}$ caused by the models of interest here have been tabulated in earlier references, see for example Refs. [10, 12]. However, for convenience, we report their explicit expressions and briefly comment on their properties in the next section.

The contactlike nonstandard interactions considered in the sequel are listed below:

a) The ADD scenario [7]. In the parameterization of Ref. [6], the exchange of such a KK tower is represented by the effective interaction:

$$
\mathcal{L}=i\frac{4\lambda}{\Lambda_H^4}T^{\mu\nu}T_{\mu\nu},\qquad \lambda=\pm 1. \tag{9}
$$

In Eq. (9), $T_{\mu\nu}$ denotes the energy-momentum tensor of the SM particles and Λ_H is an ultraviolet cut-off on the summation over the KK spectrum, expected in the (multi) TeV range. The corresponding corrections to the SM amplitudes for Bhabha scattering, see Eq. (8), read:

$$
\Delta_{\mathrm{LL},s}=\Delta_{\mathrm{RR},s}=\frac{\lambda}{\pi\alpha_{\mathrm{e.m.}}\Lambda_H^4}(u+\frac{3}{4}s),\quad \Delta_{\mathrm{LL},t}=\Delta_{\mathrm{RR},t}=\frac{\lambda}{\pi\alpha_{\mathrm{e.m.}}\Lambda_H^4}(u+\frac{3}{4}t),
$$

$$
\Delta_{\mathrm{LR},s}=-\frac{\lambda}{\pi\alpha_{\mathrm{e.m.}}\Lambda_H^4}(t+\frac{3}{4}s),\qquad \Delta_{\mathrm{LR},t}=-\frac{\lambda}{\pi\alpha_{\mathrm{e.m.}}\Lambda_H^4}(s+\frac{3}{4}t). \tag{10}
$$

b) The dimension-6 four-fermion contact interaction (CI) scenario [1]. With $\Lambda_{\alpha\beta}$ ($\alpha, \beta = \mathrm{L}, \mathrm{R}$) the "compositeness" mass scales, and δ_{ef} =1 (0) for $f = e$ ($f \neq e$):

$$\mathcal{L} = \frac{4\pi}{1+\delta_{ef}} \sum_{\alpha,\beta} \frac{\eta_{\alpha\beta}}{\Lambda^2_{\alpha\beta}} \left(\bar{e}_\alpha \gamma_\mu e_\alpha\right) \left(\bar{f}_\beta \gamma^\mu f_\beta\right), \qquad \eta_{\alpha\beta} = \pm 1, 0. \tag{11}$$

The induced deviations in Eq. (8) are:

$$\Delta_{\alpha\beta,s} = \Delta_{\alpha\beta,t} = \frac{1}{\alpha_{\mathrm{e.m.}}} \frac{\eta_{\alpha\beta}}{\Lambda^2_{\alpha\beta}}. \tag{12}$$

Rather generally, this kind of effective interactions applies to the cases of very massive virtual exchanges, such as heavy Z's, leptoquarks, *etc.*

Current experimental lower bounds on Λs are mostly derived from nonobservation of deviations at LEP and Tevatron colliders. At the 95% C.L., they are: $\Lambda_H > 1.3\,\mathrm{TeV}$ and, generically, $\Lambda_{\alpha\beta} > 10 - 15\,\mathrm{TeV}$, depending on the processes measured and the type of analysis performed [13].

c) Models with TeV^{-1}-scale extra dimensions [14, 15]. The effective interactions in contact interaction approximation for $e^+e^- \to \bar{f}f$ can be written as

$$\begin{aligned} \mathcal{L}^{\mathrm{TeV}} &= -\frac{\pi^2}{3M_C^2}[Q_e Q_f (\bar{e}\gamma_\mu e)(\bar{f}\gamma^\mu f) \\ &+ (g^e_{\mathrm{L}} \bar{e}_{\mathrm{L}} \gamma_\mu e_{\mathrm{L}} + g^e_{\mathrm{R}} \bar{e}_{\mathrm{R}} \gamma_\mu e_{\mathrm{R}})(g^f_{\mathrm{L}} \bar{f}\gamma^\mu f_{\mathrm{L}} + g^f_{\mathrm{R}} \bar{f}_{\mathrm{R}} \gamma^\mu f_{\mathrm{R}})]. \end{aligned} \tag{13}$$

The corresponding deviation can be written as

$$\Delta_{\alpha\beta,s} = \Delta_{\alpha\beta,t} = -(Q_e Q_f + g^e_\alpha\, g^f_\beta) \frac{\pi^2}{3\,M_C^2} \tag{14}$$

For the TeV^{-1}-scale extra dimension scenario the current limit, mostly determined by LEP data, is $M_C > 6.8\,\mathrm{TeV}$.

2.2 Discovery reach

The basic objects are the relative deviations of observables from the SM predictions due to the NP:

$$\Delta(\mathcal{O}) = \frac{\mathcal{O}(\mathrm{SM} + \mathrm{NP}) - \mathcal{O}(\mathrm{SM})}{\mathcal{O}(\mathrm{SM})}, \tag{15}$$

and, as anticipated, we concentrate on the polarized differential cross section, $\mathcal{O} \equiv \mathrm{d}\sigma/\mathrm{d}\cos\theta$.

To derive the constraints on the models, one has to compare the theoretical deviations from the SM predictions, that are functions of Λs, to the foreseen experimental uncertainties on the differential cross sections. To this purpose, taking the polarized angular distributions as basic observables for the analysis, $\mathcal{O} = \mathrm{d}\sigma(P^-, P^+)/\mathrm{d}z$, we introduce χ^2:

$$\chi^2(\mathcal{O}) = \sum_{\{P^-,\ P^+\}} \sum_{\text{bins}} \left(\frac{\Delta(\mathcal{O})^{\text{bin}}}{\delta\mathcal{O}^{\text{bin}}} \right)^2 . \tag{16}$$

Here, for the individual processes, the cross sections for the different initial polarization configurations are combined in the χ^2, and $\delta\mathcal{O}$ denotes the expected experimental relative uncertainty (statistical plus systematic one). As indicated in Eq. (16), we divide the angular range into bins. For Bhabha scattering, the cut angular range $|\cos\theta| < 0.90$ is divided into ten equal-size bins. Similarly, for annihilation into muon, tau and quark pairs we consider the analogous binning of the cut angular range $|\cos\theta| < 0.98$.

For the Bhabha process, we combine the cross sections with the following initial electron and positron longitudinal polarizations: $\{P^-, P^+\} = (|P^-|, -|P^+|)$; $(-|P^-|, |P^+|$; $(|P^-|, |P^+|)$; $(-|P^-|, -|P^+|)$. For the "annihilation" processes in Eq. (1), with $f \neq e, t$, we limit to combining the $(P^-, P^+) = (|P^-|, -|P^+|)$ and $(-|P^-|, |P^+|)$ polarization configurations. Numerically, we take the expected values $|P^-| = 0.8$, $|P^+| = 0.3$ and $|P^+| = 0.6$.

Regarding the ILC energy and time-integrated luminosity, we take $\sqrt{s} = 0.5$ TeV with $\mathcal{L}_{\text{int}} = 500\ fb^{-1}$, and $\sqrt{s} = 1$ TeV with $\mathcal{L}_{\text{int}} = 1000\ fb^{-1}$. The assumed reconstruction efficiencies, that determine the expected statistical uncertainties, are 100% for e^+e^- final pairs; 95% for final l^+l^- events ($l = \mu, \tau$); 35% and 60% for $c\bar{c}$ and $b\bar{b}$, respectively. The major systematic uncertainties are found to originate from uncertainties on beams polarizations and on the time-integrated luminosity: we assume $\delta P^-/P^- = \delta P^+/P^+ = 0.1\%$ and $\delta\mathcal{L}_{\text{int}}/\mathcal{L}_{\text{int}} = 0.5\%$, respectively.

As theoretical inputs, for the SM amplitudes we use the effective Born approximation [16] with $m_{\text{top}} = 175$ GeV and $m_{\text{H}} = 120$ GeV. Concerning the $\mathcal{O}(\alpha)$ QED corrections, the (numerically dominant) effects from initial-state radiation for Bhabha scattering and the annihilation processes in (1) are accounted for by a structure function approach including both hard and soft photon emission, and by a flux factor method, respectively. By a calculation

Table 1: 95% C.L. discovery reaches (in TeV). Left entry in each column refers to the unpolarized beams ($|P^-|, |P^+|$)=(0,0), right entry corresponds to ($|P^-|$,$|P^+|$)=(0.8, 0.6) at $\sqrt{s} = 1$ TeV, $\mathcal{L}_{\rm int} = 1000$ fb^{-1}, respectively.

Model	Processes							
	$e^+e^- \to e^+e^-$		$e^+e^- \to l^+l^-$		$e^+e^- \to \bar{b}b$		$e^+e^- \to \bar{c}c$	
Λ_H	9.9;	10.2	6.8;	7.2	6.8;	7.6	6.8;	7.2
Λ^{ef}_{VV}	223.3;	237.2	230.2;	254.1	196.2;	245.5	216.7;	241.4
Λ^{ef}_{AA}	133.6;	187.5	206.5;	228.0	196.6;	249.3	197.5;	220.2
Λ^{ef}_{LL}	119.3;	151.9	138.3;	176.0	163.4;	187.5	141.7;	171.8
Λ^{ef}_{RR}	114.9;	150.5	132.3;	174.6	109.4;	180.1	120.7;	171.3
Λ^{ef}_{LR}	160.0;	179.7	125.3;	161.5	126.2;	171.3	94.2;	145.4
Λ^{ef}_{RL}	$\Lambda_{RL} = \Lambda_{LR}$		125.0;	162.2	121.3;	153.1	131.8;	153.8
M_C	36.2;	38.7	51.8;	57.2	16.0;	26.8	26.8;	30.8

based on the ZFITTER code [17], other QED effects such as final-state and initial-final state emission are found, in processes $e^+e^- \to l^+l^-$ and $e^+e^- \to \bar{q}q$ ($q = c, b$), to be numerically unimportant for the chosen kinematical cuts.

The expected discovery reaches on the contactlike effective interactions are assessed by assuming a situation where no deviation from the SM predictions is observed within the experimental uncertainty. Accordingly, the corresponding upper limits on the accessible values of Λs are determined by the condition $\chi^2(\mathcal{O}) \leq \chi^2_{\rm CL}$, and we take $\chi^2_{\rm CL} = 3.84$ for a 95% C.L. In Table 1, we present the numerical results from the processes listed in the caption. Here, l^+l^- denotes the combination of $\mu^+\mu^-$ and $\tau^+\tau^-$ final states, and $\mu-\tau$ universality has been assumed for the limits on the CI mass scales.

For the Bhabha scattering, Eq. (11) envisages the existence of three independent CI models, each one contributing to individual helicity amplitudes or combinations of them, with *a priori* free, and nonvanishing, coefficients $\epsilon_{\alpha\beta} = \eta_{\alpha\beta}/\Lambda^2_{\alpha\beta}$ (basically, $\epsilon_{\rm LL}$, $\epsilon_{\rm RR}$ and $\epsilon_{\rm LR} = \epsilon_{\rm RL}$ combined with the $\pm$ signs). For other processes $e^+e^- \to \bar{f}f$ (with $f = \mu, \tau, c, b$) there are four independent CI couplings. Correspondingly, in principle, a model-independent analysis of the data should account for the situation where the full Eq. (11) is included in the expression for the cross sections. Potentially, in this case, the different CI couplings may interfere and such interference could substantially weaken the bounds. To this aim, in the case of the processes (1), ILC consid-

ered here, a possibility is offered by *initial beam polarization* to disentangle the constraints on the corresponding CI constants.

The model-independent reach on the CI couplings, and the corresponding constraints on their allowed values in the case of no effect observed, can be estimated by the method based on the covariance matrix adapted for such kind of analysis. In this approach model-independent allowed domains in the three- or four-dimensional CI parameter space to 95% confidence level are obtained from the error contours determined by the quadratic form in $\epsilon_{\alpha\beta}$ that can be written as:

$$(\epsilon_{LL}\ \epsilon_{LR}\ \epsilon_{RR})\, W^{-1} \begin{pmatrix} \epsilon_{LL} \\ \epsilon_{LR} \\ \epsilon_{RR} \end{pmatrix} = w^2, \tag{17}$$

where W^{-1} being the inverse covariance matrix, $w^2 = 7.82$ and 9.49 for processes Bhabha scattering and fermion pair production with $f = \mu, \tau, c, b$, respectively. For Bhabha scattering the quadratic form (17) defines a three-dimensional surface in the (ϵ_{LL}, ϵ_{LR}, ϵ_{RR}) parameter space. The matrix W has the property that the square roots of the individual diagonal matrix elements, $\sqrt{W_{\alpha\alpha}}$, determine the projection of the surface onto the corresponding α-parameter axis in the three-dimensional space, and has the meaning of the bound at 95% C.L. on that parameter regardless of the values assumed for the others. These model-independent limits are shown in Fig. 1 for Bhabha scattering. As an example, in Fig. 1 (right panel) we also show the planar region that is obtained from Bhabha scattering by projecting onto the plane ($\epsilon_{LL}, \epsilon_{RR}$) the 95% C.L. allowed three-dimensional surface resulting from Eq. (17). Also, Fig. 1 and Fig. 2 show the role of initial beam polarizations to increase the sensitivity of observables to CI parameters.

2.3 Identification reaches

Continuing the previous χ^2-based analysis, we now assume that deviations has been observed and are consistent with the ADD scenario (9) for some value of Λ_H. To assess the level at which the ADD model can be discriminated from the general CI model as the source of the deviations or, equivalently, to determine the "model-independent" identification reach on the effective interaction (9), we introduce in analogy with Eq. (16) the relative deviations

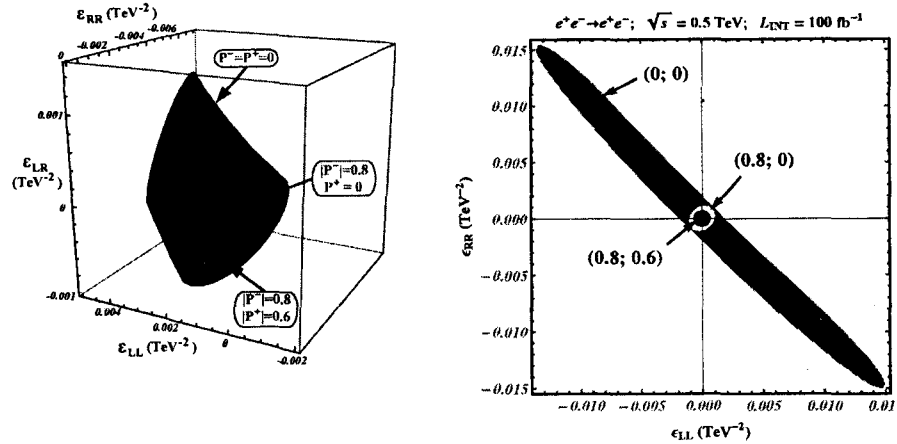

Figure 1: Left panel: 95% C.L. allowed three-dimensional surfaces obtained from Bhabha scattering at $\sqrt{s} = 500$ GeV, $\mathcal{L}_{\rm int} = 100\,{\rm fb}^{-1}$ and different values of beams polarizations $(|P^-|;|P^+|) = (0;0)$, $(0.8;0)$ and $(0.8;0.6)$. Right panel: Two-dimensional projection of the 95% C.L. allowed region for unpolarized beams ($P^- = P^+ = 0$), polarized only electrons ($P^- \neq 0$, $P^+ = 0$) and both beams polarized ($P^- \neq 0$, $P^+ \neq 0$).

$\tilde{\Delta}$ and the corresponding $\tilde{\chi}^2$:

$$\tilde{\Delta}(\mathcal{O}) = \frac{\mathcal{O}(\Lambda_{\rm LL}, \Lambda_{\rm RR}, \Lambda_{\rm RL}, \Lambda_{\rm LR}) - \mathcal{O}({\rm ADD})}{\mathcal{O}({\rm ADD})};$$

$$\tilde{\chi}^2(\mathcal{O}) = \sum_{\{P^-,\,P^+\}} \sum_{\rm bins} \left(\frac{\tilde{\Delta}(\mathcal{O})^{\rm bin}}{\tilde{\delta}\mathcal{O}^{\rm bin}} \right)^2 . \qquad (18)$$

In Eq. (18), $\tilde{\Delta}(\mathcal{O})$ depends on all Λs, and somehow represents the "distance" between the ADD and the CI model in the parameter space (Λ_H, $\Lambda_{\alpha\beta}$). Moreover, $\tilde{\delta}\mathcal{O}^{\rm bin}$ is the expected relative uncertainty referred to the cross sections that include the ADD model contributions: its statistical component is therefore determined from helicity amplitudes with the deviations (10) predicted for the given value of Λ_H. In turn, the CI contributions to the cross sections bring in the dependence of Eq. (18) on the parameters $\Lambda_{\alpha\beta}$ of Eq. (12), now considered as *all* independent. Therefore, for each of processes (1), $\tilde{\chi}^2$ is a function of λ/Λ_H^4 and in general, simultaneously of the four CI couplings $\eta_{\alpha\beta}/(\Lambda^{ef}_{\alpha\beta})^2$.

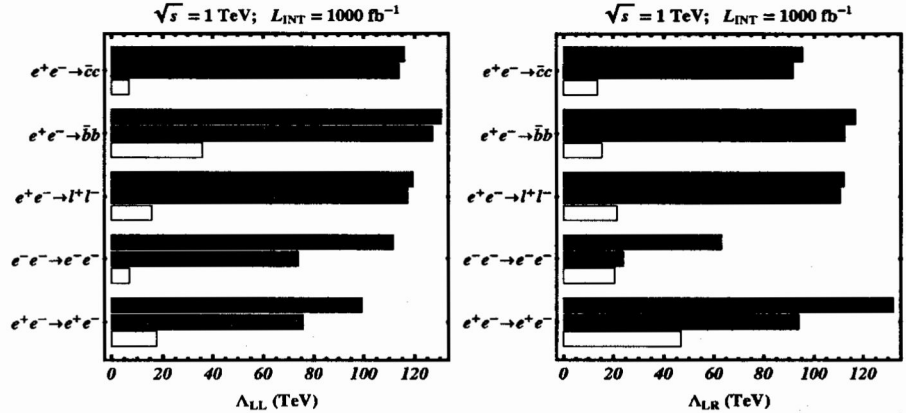

Figure 2: Model-independent discovery reaches at 95% C.L. obtained at different combinations of polarizations $(|P^-|; |P^+|)=(0; 0)$: open bars, (0.8; 0): gray bars and (0.8; 0.6): black bars.

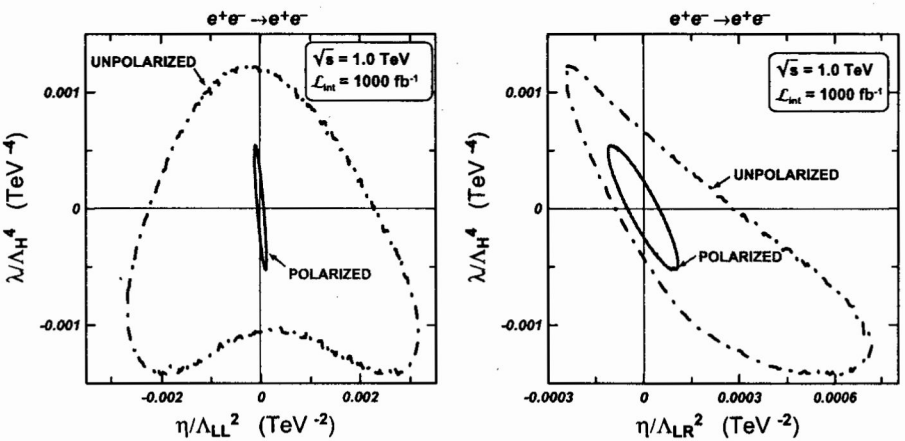

Figure 3: Two-dimensional projection of the 95% C.L. confusion region onto the planes $(\eta_{\rm LL}/\Lambda^2_{\rm LL}, \lambda/\Lambda^4_H)$ (left panel) and $(\eta_{\rm LR}/\Lambda^2_{\rm LR}, \lambda/\Lambda^4_H)$ (right panel) obtained from Bhabha scattering with unpolarized beams (dot-dashed curve) and with both beams polarized (solid curve).

In this situation we can determine *confusion regions* in the parameter space, where the CI model can be considered as consistent with the ADD

model, in the sense that it can mimic the differential cross sections of the individual processes (1) determined by the latter one. At a given C.L., these confusion regions are determined by the condition

$$\tilde{\chi}^2 \leq \chi^2_{\rm CL}. \tag{19}$$

For 95% C.L. we choose $\chi^2_{\rm CL} = 7.82$ for Bhabha scattering and $\chi^2_{\rm CL} = 9.49$ for lepton ($\mu^+\mu^-$, $\tau^+\tau^-$) and quark ($\bar{c}c$, $\bar{b}b$) pair production processes. Eq. (19) defines a four-dimensional surface enclosing a volume in the (λ/Λ_H^4, $\eta_{\rm LL}/\Lambda^2_{\rm LL}$, $\eta_{\rm RR}/\Lambda^2_{\rm RR}$, $\eta_{\rm LR}/\Lambda^2_{\rm LR}$) parameter space. In Fig. 2, we show the planar surfaces that are obtained by projecting the 95% C.L. four-dimensional surface, hence the corresponding confusion region that results from the condition $\tilde{\chi}^2 = \chi^2_{\rm CL}$.

As suggested by Fig. 2, the contour of the confusion region turns out to identify a maximal value of $|\lambda/\Lambda_H^4|$ (equivalently, a minimum value of Λ_H), for which the CI scenario can be excluded at the 95 % C.L. for any value of $\eta/\Lambda^2_{\alpha\beta}$. This value, $\Lambda_H^{\rm ID}$, is the identification reach on the ADD scenario, namely, for $\Lambda_H < \Lambda_H^{\rm ID}$ the CI scenario can be excluded as explanation of deviations from SM predictions attributed to the ADD interaction, and the latter can therefore be *identified.*

Fig. 2 shows the dramatic rôle of initial beams polarization in obtaining a restricted region of confusion in the parameter space or, in other words, in enhancing the identification sensitivity of the differential angular distributions to $\Lambda_H^{\rm ID}$. Table 2 shows the numerical results for the foreseeable "model-independent" identification reaches on Λ_H.

Table 2: 95% C.L. identification reach on the ADD model parameter Λ_H obtained from $e^+e^- \to \bar{f}f$ at $\sqrt{s} = 0.5$ TeV, $\mathcal{L}_{\rm int} = 500$ fb^{-1} with polarizations ($|P^-|$,$|P^+|$)=(0.8, 0.3) and $\sqrt{s} = 1$ TeV, $\mathcal{L}_{\rm int} = 1000 fb^{-1}$ with polarizations ($|P^-|$,$|P^+|$)=(0.8, 0.6).

Λ_H (TeV)	Process			
	$e^+e^- \to e^+e^-$	$e^+e^- \to l^+l^-$	$e^+e^- \to \bar{b}b$	$e^+e^- \to \bar{c}c$
$\sqrt{s} = 0.5$ TeV	3.2	2.6	3.4	2.9
$\sqrt{s} = 1.0$ TeV	6.5	4.7	6.2	5.4

3 LHC observables and constraints on extra dimension parameters

3.1 Center–edge asymmetry A_{CE}

At hadron colliders, lepton pairs can in the SM be produced at tree-level via the following sub-process

$$q\bar{q} \to \gamma, Z \to l^+l^-, \tag{20}$$

where we shall use $l = e, \mu$. If gravity can propagate in extra dimensions, the possibility of KK graviton exchange opens up two tree-level channels at hadron colliders in addition to the SM channels, namely

$$q\bar{q} \to G \to l^+l^-, \qquad gg \to G \to l^+l^-, \tag{21}$$

where G represents the gravitons of the KK tower.

Consider a lepton pair of invariant mass M at rapidity y (of the parton c.m. frame) and with $z = \cos\theta_{\mathrm{cm}}$, where θ_{cm} is the angle, in the c.m. frame of the two leptons, between the lepton (l^-) and the proton P_1. The inclusive differential cross section for producing such a pair, can at the LHC proton-proton collider be expressed as

$$\begin{aligned}\frac{d\sigma_{q\bar{q}}}{dM\,dy\,dz} = K\frac{2M}{s}\sum_q \{[f_{q|P_1}(\xi_1,M)f_{\bar{q}|P_2}(\xi_2,M) + \\ + \; f_{\bar{q}|P_1}(\xi_1,M)f_{q|P_2}(\xi_2,M)]\frac{d\hat{\sigma}^{\mathrm{even}}_{q\bar{q}}}{dz} + [f_{q|P_1}(\xi_1,M)f_{\bar{q}|P_2}(\xi_2,M) - \\ - \; f_{\bar{q}|P_1}(\xi_1,M)f_{q|P_2}(\xi_2,M)]\frac{d\hat{\sigma}^{\mathrm{odd}}_{q\bar{q}}}{dz}\},\end{aligned} \tag{22}$$

$$\frac{d\sigma_{gg}}{dM\,dy\,dz} = K\frac{2M}{s} f_{g|P_1}(\xi_1,M)f_{g|P_2}(\xi_2,M)\frac{d\hat{\sigma}_{gg}}{dz}. \tag{23}$$

Here, $d\hat{\sigma}^{\mathrm{even}}_{q\bar{q}}/dz$ and $d\hat{\sigma}^{\mathrm{odd}}_{q\bar{q}}/dz$ are the even and odd parts (under $z \leftrightarrow -z$) of the partonic differential cross section $d\hat{\sigma}_{q\bar{q}}/dz$, and the minus sign in the odd term allows us to interpret the angle in the parton cross section as being relative to the quark momentum (rather than P_1). Furthermore, K is a factor accounting for higher order QCD corrections (we take $K = 1.3$, which is a

typical value), $f_{j|P_i}(\xi_i, M)$ are parton distribution functions in the proton P_i, and the ξ_i are fractional parton momenta

$$\xi_1 = \frac{M}{\sqrt{s}} e^{y}, \qquad \xi_2 = \frac{M}{\sqrt{s}} e^{-y}. \tag{24}$$

We also made use of the relation $d\xi_1\, d\xi_2 = dM(2M/s)dy$ and have $M^2 = \xi_1 \xi_2 s$, with s the pp c.m. energy squared.

The center–edge and total cross sections can at the parton level be defined like for initial-state electrons and positrons [18]:

$$\hat{\sigma}_{\rm CE} \equiv \left[\int_{-z^*}^{z^*} - \left(\int_{-1}^{-z^*} + \int_{z^*}^{1} \right) \right] \frac{d\hat{\sigma}}{dz}\, dz, \quad \hat{\sigma} \equiv \int_{-1}^{1} \frac{d\hat{\sigma}}{dz}\, dz. \tag{25}$$

These will play a central role in the center–edge asymmetry at the hadron level. At this point, $0 < z^* < 1$ is just an arbitrary parameter which defines the border between the "center" and the "edge" regions.

At hadron colliders, the center–edge asymmetry can for a given dilepton invariant mass M be defined as

$$A_{\rm CE}(M) = \frac{d\sigma_{\rm CE}/dM}{d\sigma/dM}, \tag{26}$$

where we obtain $d\sigma_{\rm CE}/dM$ and $d\sigma/dM$ from (22) by integrating over z according to Eq. (25) and over rapidity between $-Y$ and Y, with $Y = \log(\sqrt{s}/M)$,

$$\frac{d\sigma}{dM} = \frac{d\sigma_{q\bar{q}}}{dM} + \frac{d\sigma_{gg}}{dM}. \tag{27}$$

For the SM contribution to the center–edge asymmetry, we see that the convolution integrals, depending on the parton distribution functions, cancel, and the result is

$$A_{\rm CE}^{\rm SM} = \tfrac{1}{2}\, z^*(z^{*2} + 3) - 1, \tag{28}$$

which is independent of M and identical to the result for e^+e^- colliders [18]. Hence, in the case of no cuts, there is a unique value, z_0^*, of z^* for which $A_{\rm CE}^{\rm SM}$ vanishes:

$$z_0^* = (\sqrt{2}+1)^{1/3} - (\sqrt{2}-1)^{1/3} \simeq 0.596, \tag{29}$$

corresponding to $\theta_{\rm cm} = 53.4°$.

The structure of the differential SM cross section is particularly interesting in that it is equally valid for a wide variety of NP models: composite-like

contact interactions, Z' models, TeV-scale gauge bosons, *etc.* Conventional four-fermion contact-interaction effects of the vector–vector kind would yield the same center–edge asymmetry as the SM. If however KK graviton exchange is possible, the tensor couplings would yield a different angular distribution, hence a different dependence of $A_{\rm CE}$ on z^*. In particular, the center–edge asymmetry would not vanish for the same choice of $z^* = z_0^*$ and, moreover, would show a non-trivial dependence on M. Thus, a value for $A_{\rm CE}$ different from $A_{\rm CE}^{\rm SM}$ would indicate non-vector exchange NP.

3.2 Identification of spin-2 and concluding remarks

We define the bin-integrated center–edge asymmetry integrated over bins i in M by introducing such an integration,

$$A_{\rm CE}(i) = \int_i \frac{d\sigma_{\rm CE}}{dM} dM \Big/ \int_i \frac{d\sigma}{dM} dM. \tag{30}$$

The deviation of the center–edge asymmetry from pure spin-1 exchange, $A_{\rm CE}^{\rm spin-1}(i)$, in each bin, and statistical uncertainty are then given as

$$\Delta A_{\rm CE}(i) = A_{\rm CE}(i) - A_{\rm CE}^{\rm spin-1}(i), \quad \delta A_{\rm CE}(i) = \sqrt{\frac{1 - A_{\rm CE}^2(i)}{\epsilon_l \mathcal{L}_{\rm int} \sigma(i)}}. \tag{31}$$

Also, we take the efficiency for reconstruction of lepton pairs, $\epsilon_l = 90\%$ and sum over $l = e, \mu$. The statistical significance, $\mathcal{S}_{\rm CE}(i)$ and χ^2 function are defined as:

$$\mathcal{S}_{\rm CE}(i) = \frac{|\Delta A_{\rm CE}(i)|}{\delta A_{\rm CE}(i)}, \quad \chi^2 = \sum_i [\mathcal{S}_{\rm CE}(i)]^2, \tag{32}$$

where i runs over the different bins in M.

At the LHC, with 100 fb^{-1}, we require $M > 400$ GeV and divide the data into 200 GeV bins as long as the number of events in each bin, $\epsilon_l \mathcal{L}_{\rm int} \sigma(i)$, is larger than 10. Therefore, the number of bins will depend on the magnitude of the deviation from the SM. We impose angular cuts relevant to the LHC detectors, in order to account for the fact that detectors have a region of reduced or no efficiency close to the beam direction. The lepton pseudorapidity cut is $|\eta| < \eta_{\rm cut} = 2.5$ for both leptons, and in addition to the angular cuts, we impose on each lepton a transverse momentum cut $p_\perp > p_\perp^{\rm cut} = 20$ GeV.

In Table 3 we summarize the results including the *identification* reach on cut-off scale Λ_H at the LHC and ILC. Table 3 shows the identification reach

Table 3: Identification reach on Λ_H (in TeV) at 95% C.L. from $p + p \to l^+l^- + X$ at LHC and from $e^+e^- \to \bar{f}f$ $(f = e, \mu, \tau, c, b)$ at ILC.

Collider	$\lambda = +1$	$\lambda = -1$
LHC 100 fb^{-1}	4.8	5.0
LHC 300 fb^{-1}	5.4	5.9
ILC(0.5 TeV) 500 fb^{-1}	4.8	
ILC(1 TeV) 1000 fb^{-1}	8.8	

on Λ_H obtained from combination of all final fermions $(f = e, \mu, \tau, c, b)$ in process $e^+e^- \to \bar{f}f$ at ILC. To compare the potential of the LHC and ILC to identify graviton exchange signals, we present in Table 3 the identification reach on the mass scale Λ_H at different options of colliders. We see that LHC has advantage over ILC with $\sqrt{s} = 0.5$ TeV, while ILC with $\sqrt{s} = 1$ TeV allows to substantially improve those bounds obtained at LHC.

Acknowledgment
This work is partially supported by the ICTP through the OEA-Affiliated Centre-AC88.

References

[1] Eichten, E., Lane, K., and Peskin, M.E., *Phys. Rev. Lett.* **50**, 811-814 (1983).

[2] For reviews see, *e.g.*: Hewett, J.L., and Rizzo, T.G., *Phys. Rept.* **183**, 1-193 (1989);
Leike A., *Phys. Rept.* **317**, 143-250 (1999).

[3] Buchmuller, W., Ruckl, R., and Wyler, D., *Phys. Lett.* B **191**, 442-449 (1987).

[4] Rizzo, T.G., *Phys. Rev.* D **59**, 113004 (1999).

[5] Gounaris, G.J., Papadamou, D.T., and Renard, F.M., *Phys. Rev.* D **56**, 3970-3979 (1997).

[6] Hewett, J. L., *Phys. Rev. Lett.* **82**, 4765-4768 (1999).

[7] Arkani-Hamed, N., Dimopoulos, S., and Dvali, G.R., *Phys. Lett.* B **429**, 263-272 (1998).

[8] Pankov, A.A., and Paver, N., *Phys. Rev.* D **72**, 035012 (2005).

[9] Pankov, A.A., and Paver, N., *Eur. Phys. J.* C **29**, 313-323 (2003).

[10] Pankov, A.A., Paver, N., and Tsytrinov, A.V., *Phys. Rev.* D **73**, 115005 (2006).

[11] Pankov, A.A., Paver, N., and Tsytrinov, A.V., *Phys. Rev.* D **75**, 095004 (2007).

[12] Cullen, S., Perelstein, M., and Peskin, M.E., *Phys. Rev.* D **62**, 055012 (2000).

[13] Yao, W.M.*et al.* [Particle Data Group], *J. Phys.* G **33**, 1-1232 (2006).

[14] Cheung, K.M., and Landsberg, G., *Phys. Rev.* D **65**, 076003 (2002).

[15] Rizzo, T.G., and Wells, J.D., *Phys. Rev.* D **61**, 016007 (2000).

[16] Altarelli, G., Casalbuoni, R., Dominici, D., Feruglio, F., and Gatto, R., *Nucl. Phys.* B **342**, 15-60 (1990).

[17] Bardin, D. Y., Christova, P., Jack, M., Kalinovskaya, L., Olchevski,A., Riemann, S., and Riemann, T., *Comput. Phys. Commun.* **133**, 229-395 (2001).

[18] Osland, P., Pankov, A.A., and Paver, N., *Phys. Rev.* D **68**, 015007 (2003).